M-graphene: a metastable two-dimensional carbon allotrope

Chunlei Kou[1] , Yuanye Tian[2] , Miao Zhang[2,3], Eva Zurek[3], Xin Qu[4], XiaoyuWang[3],
Ketao Yin[5], Yan Yan[3,6], Lili Gao[2] , Mingchun Lu[7] and Wensheng Yang[1]

[1]College of Chemistry, Jilin University, Changchun 130012, People's Republic of China

[2]Department of Physics, School of Sciences, Beihua University, Jilin 132013, People's Republic of China

[3]Department of Chemistry, State University of New York at Buffalo, Buffalo, NY 14260-3000, United States of America

[4]Key Laboratory of Functional Materials Physics and Chemistry of the Ministry of Education, Jilin Normal University, Changchun 130103, People's Republic of China

[5]School of Physics and Electronic Engineering, Linyi University, Linyi, Shandong 276005, People's Republic of China

[6]School of Sciences, Changchun University, Changchun 130022, People's Republic of China

[7]Department of Aeronautical Engineering Professional Technology, Jilin Institute of Chemical Technology, Jilin 132102,People's Republic of China

E-mail: zhangmiaolmc@126.com, ezurek@buffalo.edu and wsyang@jlu.edu.cn

Keywords: 2D carbon allotrope, first-principles calculations, anode material for Li-ion batteri

Abstract

Ever since the exfoliation of graphene, two-dimensional (2D) atomic layers derived from bulk materials have received significant attention because of their fascinating properties, as well as their potential for technological applications. In this work, a metastable planar 2D carbon allotrope composed of 5 + 7 rings (dubbed M-graphene) was predicted via an unbiased crystal structure prediction algorithm based upon the particle swarm methodology and studied via first-principles calculations. Computations show that M-graphene is not only dynamically stable, but it can also withstand temperatures as high as 2000 K. Our simulations reveal that it is a promising candidate as an anode material for Li-ion batteries (LIBs), because of the relatively low diffusion energy barrier of Li (0.338 eV), open-circuit potential (0.029 V) and high lithium-storage capacity (279 mAh g^{-1}). This work may be useful for designing novel 2D carbon-based materials.

Introduction

It is well known that two dimensional (2D) materials are being intensely investigated to advance basic science, and because of their potential technological applications that arise from their unique structural, physical, and chemical properties. Graphene, a zero-gap semi-metal arranged in a honeycomb lattice, was successfully isolated from graphite by using a micromechanical cleavage method and has prompted researchers to explore other novel 2D materials with fascinating properties [1–3]. However, during the growth or processing of graphene, structural defects always appear in the perfect honeycomb lattice. One example is a Stone–Wales defect [4], which is a crystallographic defect that involves the change of connectivity of two π-bonded carbon atoms, leading to their rotation by 90◦ with respect to the midpoint of their bond, which can convert four hexagons into two pentagons and two heptagons.

Although the presence of defects breaks the perfect symmetry of the graphene lattice and influences some of its properties, such as reducing the mobility of charge carriers [5, 6], defects can be beneficial for other properties. For example, defects can increase the reactivity of graphene and can be used to tune its electronic properties in catalytic applications. Therefore, introducing non-hexagonal defects into hexagonal lattices has become an effective method to reconstruct carbon atoms, and improve electronic properties.

Extensive work has been dedicated to the exploration of the unique crystal structures of novel 2D carbon allotropes with enhanced mechanical and electrical performance [7–40]. The proposed structures have been constructed from polygons containing different numbers of sides, such as 5 rings [7], 5 + 7 rings [8–10], 4 + 8 rings [11], 5 + 6 + 7 rings [9, 12–16],4 + 6 + 8 rings [17–21], and 4 + 5 + 6 + 8 + 10 rings [22]. However, the synthesis of these theoretically proposed 2D carbon allotropes with improved properties is challenging. Therefore, designing and exploring novel 2D carbon allotropes that could be synthesized is interesting and worthwhile.

In this work, we used first-principles calculations to study a metastable planar 2D carbon allotrope, dubbed M-graphene, which has similar topological characteristics with M-carbon [41] (a superhard monoclinic polymorph of carbon that has been synthesized [42–44], and whose hardness and bulk modulus are comparable to those of diamond). The topology of M-graphene is reminiscent of the structures proposed earlier by the bond rotation algorithm [8], the creation of Stone–Wales-type defects on the graphene sheet that transforms pyrene-like rings into two pairs of heptagons and pentagons [9], as well as 5 + 7 graphene [10]. This planar carbon allotrope is 0.23 eV/atom higher in energy compared to graphene, and energetically favorable compared to many previously proposed carbon allotropes, suggesting that it could be synthesized in experiment. Moreover, our results show that M-graphene could be an anode material for Li-ion batteries (LIBs) from its relatively low diffusion energy barrier (0.338 eV), open-circuit potential (0.029 V) and high lithium-storage capacity (279 mAh g^{-1}).

2. Methods

The structure searches were performed using the CALYPSO crystal structure prediction method [45, 46], which is an efficient algorithm that can be used to predict a wide variety of stable and metastable materials. Our CALYPSO runs were normally stopped after 50 generations, and each generated structure was optimized four times. The geometry optimizations and electronic structure calculations were performed using density functional theory (DFT) as implemented in the Vienna *ab initio* simulation package (VASP) [47]. We used the Perdew–Burke–Ernzerhof [48] generalized gradient approximation, coupled with projector augmented wave (PAW) potentials [49] and an 800 eV energy cutoff where the $2s^2 2p^2$ electrons of C were treated explicitly. A Monkhorst–Pack 5 × 7 × 1 k-point mesh produced enthalpies well converged to below 1 meV/atom. When the forces on the atoms were less than 0.001 eV Å^{-1}, the structure was deemed to be relaxed. A vacuum distance of ~15 Å in the direction perpendicular to the monolayer was used, so that the interlayer interactions were egligible. To check the dynamical stability, the phonon spectra were computed using the finite displacement method as implemented in the Phonopy code [50]. First-principles molecular dynamics (MD) simulations under the canonical (*NVT*) ensemble were performed to examine the thermal stability. The climbing-image nudged elastic band (CI-NEB) [51] method was applied to determine the diffusion barriers of Li adatoms on the surface of M-graphene. The bonding of select phases was further analyzed by calculating the crystal orbital Hamilton populations (COHP) and the negative of the COHP integrated to the Fermi level (-ICOHP) using the LOBSTER package [52].

3. Results and discussion

3.1. 2D crystal structure of M-graphene

When graphite is compressed at ambient temperatures it undergoes a structural phase transition above 14 GPa, which has been characterized by changes in the electrical resistivity [53, 54], Raman modes [42, 55, 56], x-ray diffraction patterns [43, 57, 58], and hardness [43]. Various crystal structure prediction techniques were employed to propose a candidate whose computed properties agreed with those measured for the newly synthesized material [41, 59–67]. Based upon a comparison of the measured and calculated x-ray diffraction patterns and equations of states, as well as the energy barriers obtained using molecular-dynamics transition path sampling simulations [44, 68], M-carbon was put forward as the most likely species formed from the cold-compression of graphite [41]. M-carbon is made exclusively of three-dimensional *sp*3 hybridized covalent bonds with 5 + 7 membered rings, as shown in figure 1(a). Its hardness and bulk modulus were calculated to be 83.1 and 431.2 GPa, respectively, which is comparable to those of diamond [41].

We performed variable-cell structure prediction search using the CALYPSO methodology for simulation cells up to 32 carbon atoms at ambient pressure, and found an energetically favored stable planar carbon sheet consisting both of pentagons and heptagons (denoted as M-graphene, space group *Cmmm*, 16 atoms/cell), which has the similar topology as that of single-sheet planar carbon pentaheptite [8], as well as M-carbon, as shown in figure 1(b). At ambient pressure its optimized lattice constants are $a = 7.473$ Å and $b = 5.858$ Å. By symmetry analysis, the atoms in the unit cell of M-graphene can be divided into three sets of inequivalent atoms, with carbon occupying the 8*q* (0.658, 0.275, 0.5), 4*h* (0.906, 0, 0.5), and 4*j* (0, 0.379, 0.5) Wyckoff positions.

The planar density of M-graphene is calculated to be 0.365 atom Å^{-2} , which is slightly less than the value for graphene, 0.380 atom Å^{-2} , but larger than the value for graphdiyne (0.232 atom Å^{-2}). This suggests that the total energy of M-graphene should be higher than that of graphene, but lower than that of graphdiyne. The bond angles in M-graphene range from 105° to 139° , and are distinctly different from the 120° found within graphene. This also suggests that the strain in M-graphene is higher than that in graphene, and likely leads to an increase in the total energy.

There are five different C–C bond lengths in M-graphene, whose distances are all in-line with values expected for *sp*2 hybridized bonding, as shown in table 1. Except for the C2–C3 bond, the other four bond lengths are smaller than that of graphene (1.424 Å). Generally speaking, the bond lengths in the heptagons are closest to that of graphene, whereas the C–C bond belonging to two pentagons (C5–C6) is the shortest (1.392 Å), and one of the C–C bonds belonging to a pentagon and a heptagon (C2–C3) is the longest (1.491 Å).

To analyze the bonding further we calculated the crystal orbital Hamilton populations (COHP) and the negative of the COHP integrated to the Fermi level (-ICOHP), which are also provided in table 1. The bond strengths in M-graphene were computed to be similar to those within graphene, further corroborating the sp^2 bonding in this novel 2D sheet. The bond belonging to two heptagons was the strongest (with an -ICOHP of 11.16 eV), and the shortest and longest bonds, discussed above, were the weakest with -ICOHPs of 9.74 eV and 9.43 eV, espectively.

3.2. Thermal and dynamical stability

To investigate the thermodynamic stability of M-graphene, its total energy was calculated and compared with other well-known 2D carbon allotropes, as presented in figure 2. The energy of M-graphene is 0.23 eV/atom higher than that of graphene, and 0.54 eV/atom lower than that of graphdiyne, which was successfully synthesized in 2010 [69]. The results show that although M-graphene is metastable compared to graphene, it is more energetically favorable than the synthesized graphdiyne, suggesting that M-graphene could also potentially be synthesized in experiment. Due to the strong sp^3 covalent bonds in M-carbon, it is impossible to directly exfoliate M-graphene from M-carbon by mechanical exfoliation. However, M-graphene might be obtained via chemical techniques, such as epitaxial growth, colloidal suspension, and unconventional methods [70–72].

In order to further confirm the metastability of M-graphene, calculations were performed to obtain its phonon band structure. As shown in figure 3(a), no imaginary phonon modes are present throughout the whole Brillouin zone, indicating that M-graphene is dynamically stable. The highest phonon frequency is 1632 cm^{-1}, which is a little larger than the highest mode present in graphene (~1600 cm^{-1}) [73], suggesting that this mode could potentially be used as a spectroscopic signature to help experimentally characterize the material. At the Γ-point, the highest frequency vibrational modes are 1573 cm^{-1} and 1556 cm^{-1} for M-graphene and graphene, respectively.

We also performed first-principles molecular dynamics (MD) simulations to examine the thermal stability using the canonical NVT ensemble (which keeps the number of particles, volume, and temperature constant) within a $2 \times 3 \times 1$ supercell. The MD calculations were performed at temperatures of 300, 1000 and 2000 K, as shown in figure 4. Each simulation consisted of 10 000 time steps with a time step of 1 fs. None of the C–C bonds broke during the simulations. The sheets did not stay planar however, and the deviation from planarity increased at higher temperatures. These results reveal that M-graphene is metastable, and it possesses outstanding thermal stability at least up to 2000 K.

3.3. Potential application as an anode material for Li-ion batteries

It is well known that graphene is a zero band-gap semi-metal, and its conduction and valence bands meet at the Dirac points. The calculated electronic band structure of M-graphene at ambient pressure is shown in figure 3(b), indicating that M-graphene is metallic.

The stability and intrinsic metallicity of M-graphene makes it a promising anode material for LIBs. To explore this potential application, we investigated the electrochemical properties of M-graphene. We first selected some inequivalent high symmetry adsorption sites, namely, three top sites (T1 ~ T3), five bridge sites (B1 ~ B5), and two hollow sites (H1 ~ H2), as shown in figure 5(a), then deposited a single Li atom on each adsorption site of a 2 × 2 supercell. Geometry optimizations indicate the most favorable Li adsorption site resides on the center of the carbon rings, and the calculated adsorption energies for the H1, and H2 sites are 0.548 and 0.493 eV, respectively. The adsorption energy is defined as [12]:

$$Ea = (E_{\mathrm{M+Li}} - E_{\mathrm{M}} - \mathrm{n}E_{\mathrm{Li}})/n \quad (1)$$

where Ea is the adsorption energy, EM+Li and EM are the total energies of the M-graphene supercell after and before Li adsorption, ELi represents the energy per Li atom in the bulk Li metal, and n is the number of adsorbed Li atoms. In this calculation, we did not consider the van der Waals (vdW) contribution, since the weak vdW interactions are not as important in single-layer systems as they are in layered crystals [74]. Because the magnitude of the adsorption energy is the largest at the H1 site, this is the most preferential binding site. Furthermore, the Bader charge analysis [75] shows that the charge transfer from Li to M-graphene is ~0.89e for all cases.

We next performed climbing-image nudged elastic band (CI-NEB) [51] calculations to evaluate the mobility of Li atoms on M-graphene. The three possible migration pathways of Li considered are from one H1 site to another H1 site along the paths shown in figure 5(b). The energetics of the reaction pathways are presented in figure 5(c). The migration barrier along a path parallel to the a axis is 0.366 eV, and the migration barriers of the paths parallel to the b axis are 0.366 and 0.338 eV. The data shows the migration barrier in M-graphene is comparable to the value calculated for graphene (0.31 eV) [76]. The low-energy-migration barrier of in-plane Li diffusion indicates good charge-discharge rates of M-graphene if it was to be used as an anode material.

We also explored the Li storage capacity of M-graphene by evaluating the binding energy of a number of configurations with a $\mathrm{Li}x\mathrm{C}64$ stoichiometry (x = 1, 2, 4, 8, 12, 16). The Li adsorption energy reaches 0.029 eV/atom when the Li concentration reaches LiC8 (x = 8) and the two Li atoms are adsorbed to the center of the heptagons. The maximum theoretical specific capacity can reach 279 mAh g^{-1}, much larger than that of 112 mAh g^{-1} [77] in graphene anode materials. We then computed the average open-circuit voltage (OCV) by using the following equation:

$$\mathrm{OCV} = (E_{\mathrm{M}} + xE_{\mathrm{Li}}\ E_{\mathrm{M+Li}})/xe \quad (2)$$

the computed average OCV is 0.548 V for a stoichiometry of LiC_{64}. As the concentration increases to LiC_8, the OCV decreases to 0.029 V. The low average open-circuit voltage is beneficial to the over all voltage of the cell, which provides a favorable operating voltage for high-capacity lithium batteries. According to the low Li migration barrier, as well as the high lithium-storage capacity and low OCV values, we may expect M-graphene to be a promising material for applications in LIB anodes.

4. Conclusion

In conclusion, we predicted a planar 2D carbon material composed of 5 + 7 rings with the *Cmmm* space group via structure prediction simulations. We dubbed this 2D material M-graphene because it possesses the same topological characteristics as that of bulk M-carbon, which has been synthesized previously under high pressure. The energy of M-graphene is 0.23 eV/atom higher than that of graphene, and 0.54 eV/atom lower than that of synthesized graphdiyne, making it a metastable phase. Phonon calculations confirm that it is dynamically stable, and MD simulations show that it can withstand temperatures up to 2000 K. Moreover, first principles calculations show that the diffusion of lithium on M-graphene has a low migration barrier (0.338 eV), and the material has a low open-circuit voltage (0.029 V). The maximum lithium-storage structure of M-graphene is LiC_8, when adsorption to only one side of a single layer is considered, which corresponds to a theoretical capacity of 279 mAh g^{-1} . M-graphene provides a promising new high-performance metallic carbon allotrope anode material. Our study may open a new route to creating 2D carbon materials, which can be used in electronic devices, and motivate experimental efforts to synthesize new 2D carbon allotropes.

Acknowledgments

This research was supported by the Natural Science Foundation of China under Grant Nos. 11504007, 11747007, 61504002, 11404035, 11904148, and the Scientific and Technological Research Project of the ‘13th Five-Year Plan’ of Jilin Provincial Education Department under Grant Nos. JJKH20200031KJ, 2016049 and JJKH20180941KJ. The work was also supported by the Foster Program of Youth Research Innovation Team in Beihua University. E. Z. acknowledges the NSF (DMR-1827815) for financial support.

References

[1] Novoselov K S, Geim A K, Morozov S V, Jiang D A, Zhang Y, Dubonos S V, Grigorieva I V and Firsov A A 2004 *Science* 30 666

[2] Rao C N R, Sood A K, Subrahmanyam K S and Govindaraj A 2009 *Angew. Chem. Int. Ed.* 48 7752

[3] Allen M J, Tung V C and Kaner R B 2010 *Chem. Rev.* 110 32

[4] Stone A J and Wales D 1986 *Chem. Phys. Lett.* 128 501

[5] Haskins J, Kinaci A, Sevik C, Sevinçli H, Cuniberti G and Ca˘gin T 2011 *ACS Nano* 5 3779

[6] Tsen A W, Brown L, Levendorf M P, Ghahari F, Huang P Y, Havener R W, Ruiz-Vargas C S, Muller D A, Kim P and Park J 2012 *Science* 336 1143

[7] Zhang S, Zhou J, Wang Q, Chen X, Kawazoe Y and Jena P 2015 *Proc. Natl. Acad. Sci.* 112 2372

[8] Crespi V H, Benedict L X, Cohen M L and Louie S G 1996 *Phys. Rev.* B 53 R13303

[9] Terrones H, Terrones M, Hern´andez E, Grobert N, Charlier J C and Ajayan P M 2000 *Phys. Rev. Lett.* 84 1716

[10] Belenkov M E, Chernov V M, Belenkov E A and Morilova V M 2018 *IOP Conf. Ser. Mater. Sci. Eng.* 447 012005

[11] Liu Y, Wang G, Huang Q, Guo L and Chen X 2012 *Phys. Rev. Lett.* 108 225505

[12] Li X, Wang Q and Jena P 2017 *J. Phys. Chem. Lett.* 8 3234

[13] Wang Z, Zhou X F, Zhang X, Zhu Q, Dong H, Zhao M and Oganov A R 2015 *Nano Lett.* 15 6182

[14] Liu W, Zhao L, Zurek E, Xia J, Zheng Y H, Lin H Q and Liu J Y 2019 *Npj Comput. Mater.* 5 1

[15] Yin H C, Shi X Z, He C Y, Martinez-Canales M, Li J, Pickard C J, Tang C, Ouyang T, Zhang C X and Zhong J X 2019 *Phys. Rev.* B 99 041405

[16] Lusk M T and Carr L D 2009 Carbon 47 2226

[17] Rong J, Dong H, Feng J, Wang X, Zhang Y, Yu X and Zhao Z 2018 Carbon 135 21

[18] Hudspeth M A, Whitman B W, Barone V and Peralta J E, 2010 ACS Nano 4 4565

[19] Wang X Q, Li H D and Wang J T 2013 Phys. Chem. Chem. Phys. 15 2024

[20] Hu M, Shu Y, Cui L, Xu B, Yu D L and He J L 2014 Phys. Chem. Chem. Phys. 16 18118

[21] Xu L C, Wang R Z, Miao M S, Wei X L, Chen Y P, Yan H, Lau W M, Liu L M and Ma Y M 2014 Nanoscale 6 1113

[22] Wang X, Feng Z H, Rong J, Zhang Y N, Zhong Y, Feng J, Yu X H and Zhan Z L 2019 Carbon 142 438

[23] Liu J W, Yu G T, Huang X R and Chen W 2020 2D Mater. 7 015015

[24] Wang S J, Li J G, Zhu X and Wang M, 2019 Carbon 143 517

[25] Wang S W, Yang B C, Chen H Y and Ruckenstein E 2018 J. Mater. Chem. A 6 6815

[26] Zurek E, Pickard C J and Autschbach J 2008 J. Phys. Chem. C 112 11744

[27] Malko D, Neiss C, Viñes F and Görling A 2012 Phys. Rev. Lett. 108 086804

[28] Zhang X, Wei L, Tan J and Zhao M 2016 Carbon 105 323

[29] Appelhans D J, Lin Z and Lusk M T 2010 Phys. Rev. B 82 073410

[30] Mandal B, Sarkar S, Pramanik A and Sarkar P 2013 Phys. Chem. Chem. Phys. 15 21001

[31] Song Q, Wang B, Deng K, Feng X L, Wagner M, Gale J D, Müllen K and Zhi L J 2013 J. Mater. Chem. C 1 38
[32] Brunetto G, Santos B I, Autreto P A S, Machado L D, Dos Santos R P B and Galvao D S 2012 J. Phys. Chem. C 116 12810
[33] Borlido P, Steigemann C, Lathiotakis N N, Marques M A L and Botti S 2017 2D Mater. 4 045009
[34] Su C, Jiang H and Feng J 2013 Phys. Rev. B 87 075453
[35] Zhao L, Liu W, Yi W C, Hu T, Khodaqholian D, Gu F L, Lin H Q, Zurek E, Zheng Y H and Miao M S 2020 Nanoscale (https://doi.org/10.1039/C9NR08069D)
[36] Lu H and Li S D 2013 J. Mater. Chem. C 1 3677
[37] Narita N, Nagai S, Suzuki S and Nakao K 1998 Phys. Rev. B 58 11009
[38] Zhao M, Dong W and Wang A 2013 Sci. Rep. 3 3532
[39] Sharma B R, Manjanath A and Singh A K 2014 Sci. Rep. 4 7164
[40] Cai Y, Guo Y, Jiang B and Lv Y 2017 Sci. Rep. 7 14948
[41] Li Q, Ma Y M, Oganov A R, Wang H B, Wang H, Xu Y, Cui T, Mao H K and Zhou G T 2009 Phys. Rev. Lett. 102 175506
[42] Xu J, Mao H K and Hemley R J 2002 J. Phys. Condens. Matter 14 11549
[43] Mao W L, Mao H K, Eng P J and Trainor T P 2003 Science 302 425
[44] Wang Y, Panzik J E, Kiefer B and Lee K K M 2012 Sci. Rep. 2 520
[45] Wang Y C, Lv J, Zhu L and Ma Y M 2010 Phys. Rev. B 82 094116
[46] Wang Y C, Miao M S, Lv J, Zhu L, Yin K T, Liu H Y and Ma Y M 2012 J. Chem. Phys. 137 224108
[47] Kresse G and Furthmüller J 1996 Phys. Rev. B 54 11169
[48] Perdew J P, Burke K and Ernzerhof M 1996 Phys. Rev. Lett. 77 3865
[49] Blöchl P E 1994 Phys. Rev. B 50 17953
[50] Togo A, Oba F and Tanaka I 2008 Phys. Rev. B 78 134106
[51] Henkelman G B, Uberuaga P and J´onsson H 2000 J. Chem. Phys. 113 9901
[52] Maintz S, Deringer V L, Tchougr´eeff A L and Dronskowski R 2016 J. Comput. Chem. 37 1030
[53] Bundy F P and Kasper J S 1967 J. Chem. Phys. 46 3437
[54] Patterson J R, Catledge S A, Vohra Y K, Akella J and Weir S T 2000 Phys. Rev. Lett. 85 5364
[55] Goncharov A F, Makarenko I N and Stishov S M 1989 Sov. Phys. JETP 69 380
[56] Hanfland M, Beister H and Syassen K 1989 Phys. Rev. B 39 12598
[57] Zhao Y and Spain I L 1989 Phys. Rev. B 40 993
[58] Yagi T, Utsumi W, Yamakata M, Kikegawa T and Shimomura O 1992 Phys. Rev. B 46 6031
[59] Wang J T, Chen C F and Kawazoe Y 2011 Phys. Rev. Lett. 106 075501
[60] Zhu Q, Zeng Q F and Oganov A R 2012 Phys. Rev. B 85 201407(R)
[61] Niu H Y, Chen X Q, Wang S B, Li D Z, Mao W L and Li Y Y 2012 Phys. Rev. Lett. 108 135501
[62] He C Y, Sun L Z, Zhang C X, Peng X Y, Zhang K W and Zhong J X 2012 Solid State Commun. 152 1560
[63] Umemoto K, Wentzcovitch R M, Saito S and Miyake T 2010 Phys. Rev. Lett. 104 125504

[64] Li D, Bao K, Tian F B, Zeng Z W, He Z, Liu B B and Cui T 2012 Phys. Chem. Chem. Phys. 14 4347

[65] Zhao Z S et al 2012 J. Am. Chem. Soc. 134 12362

[66] Zhang M, Liu H Y, Du Y H, Zhang X X, Wang Y C and Li Q 2013 Phys. Chem. Chem. Phys. 15 14120

[67] Zhao Z S, Xu B, Zhou X F, Wang L M, Wen B, He J L, Liu Z Y, Wang H T and Tian Y J 2011 Phys. Rev. Lett. 107 215502

[68] Boulfelfel S E, Oganov A R and Leoni S, 2012 Sci. Rep. 2 471

[69] Li G X, Li Y L, Liu H B, Guo Y B, Li Y J and Zhu D B 2010 Chem. Commun. 46 3256

[70] Park S and Ruoff R S 2009 Nat. Nanotechnol. 4 217

[71] Allen M J, Tung V C and Kaner R B 2009 Chem. Rev. 110 132

[72] Lee B J, Yu H Y and Jeong G H 2010 Nanoscale Res. Lett. 5 1768

[73] Liu F, Ming P and Li J 2007 Phys. Rev. B 76 064120

[74] Yildirim H, Kinaci A, Zhao Z J, Chan M K Y and Greeley J P 2014 Acs Appl. Mater. Interfaces 6 21141

[75] Sanville E, Kenny S D, Smith R and Henkelman G 2007 J. Comput. Chem. 28 899

[76] Fan X, Zheng W T and Kuo J L 2012 ACS Appl. Mater. Interfaces 4 2432

[77] Pollak E, Geng B S, Jeon K J, Lucas I T, Richardson T J, Wang F and Kostecki R 2010 Nano Lett. 10 3386

Table 1. Calculated bond lengths (Å) and -ICOHP/bond (eV/bond) within M-graphene and graphene.

	Bond	Bond length (Å)	-ICOHP/ bond (eV/bond)	Average -ICOHP/ bond (eV/bond)
M-graphene	C1–C2	1.416	11.16	10.20
	C2–C3	1.491	9.43	
	C3–C4	1.399	10.69	
	C4–C5	1.404	10.01	
	C5–C6	1.392	9.74	
Graphene	C–C	1.424	10.07	10.07

Figure Caption

Figure1. (a) Top and side view of the crystal structure of M-carbon. (b) Top and side view of the atomic configuration of M-graphene. Blue, red, and green balls represent inequivalent carbon atoms.

Figure 2. Area dependence of the total energy per atom for graphene, penta-graphene, ψ-graphene, graphdiyne, net-Y and M-graphene. A_0 is the equilibrium area we calculate for the given carbon allotrope at ambient pressure.

Figure 3. Calculated phonon dispersion curve (a) and band structure of M-graphene (b). The dashed line marks the Fermi energy, EF. Bands are plotted along the high-symmetry lines of the Brillouin zone.

Figure 4. Snapshots taken from the molecular dynamics simulations of M-graphene at different temperatures.

Figure 5. (a) Li adsorption sites on M-graphene. Red, green and blue dots represent the top, bridge and hollow sites, respectively. (b) The three possible migration paths, and (c) the migration barrier of Li atom diffusion on M-graphene.

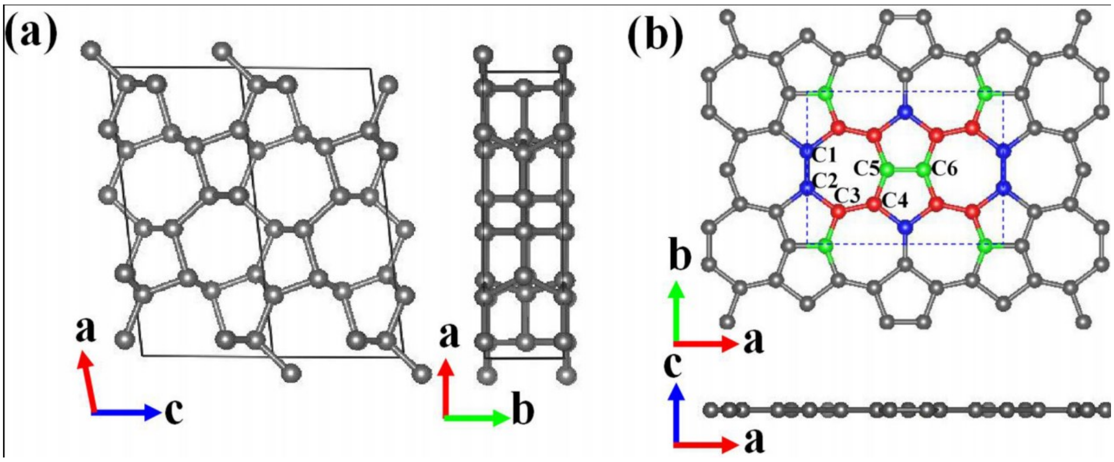

Figure 1

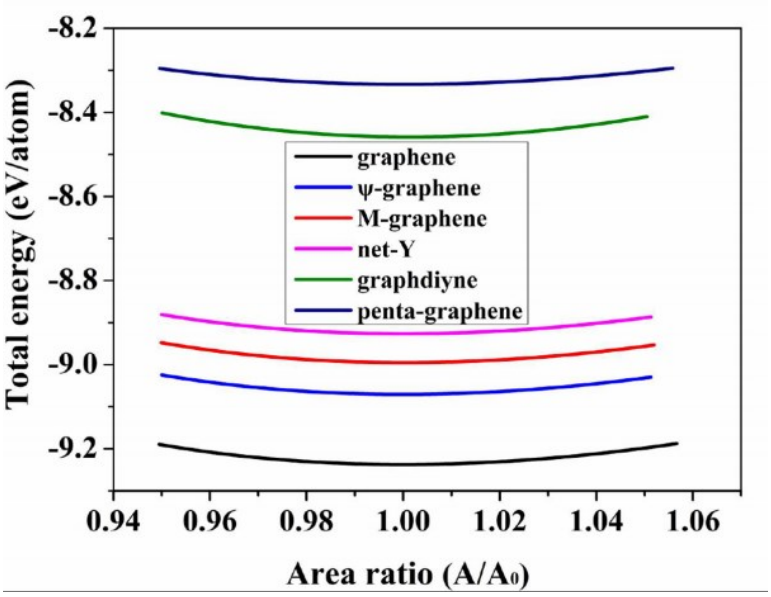
-8.2
-8.4
-8.6
-8.8
-9.0
-9.2
Total energy (eV/atom)
graphene
ψ-graphene
M-graphene
net-Y
graphdiyne
penta-graphene
0.94
0.96
0.98
1.00
1.02
1.04
1.06
Area ratio (A/A0)

Figure 2

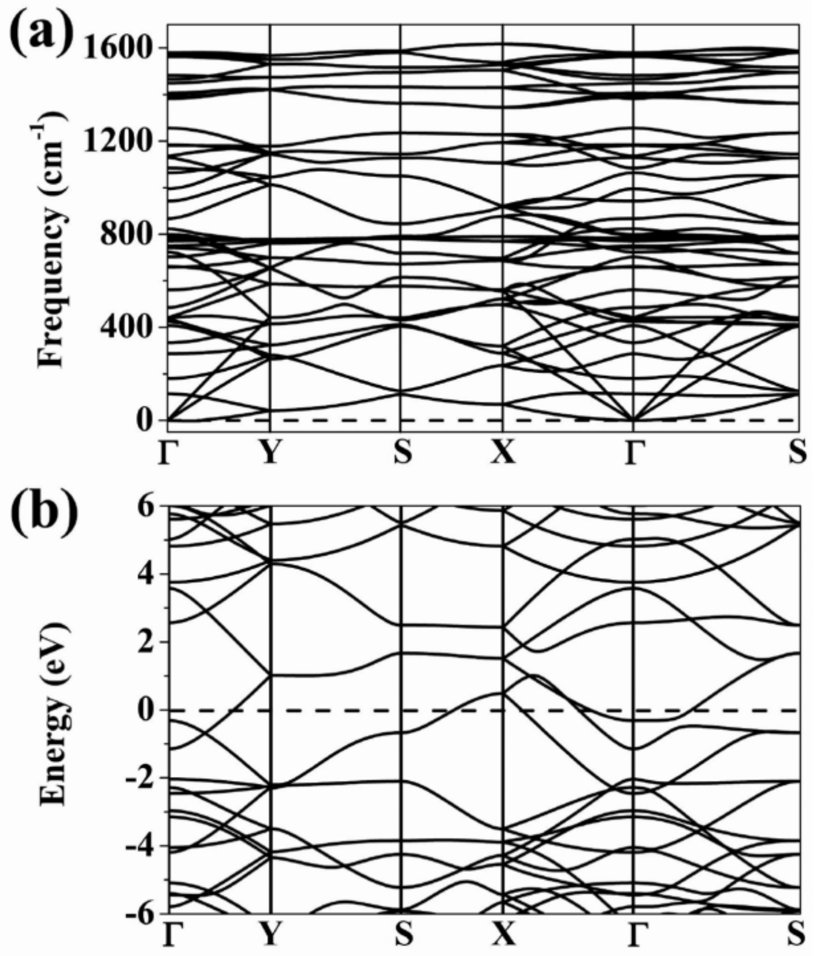
(a)
Frequency (cm^{-1})
1600
1200
800
400
0
Γ
Y
S
X
Γ
S
(b)
Energy (eV)
6
4
2
0
-2
-4
-6
Γ
Y
S
X
Γ
S

Figure 3

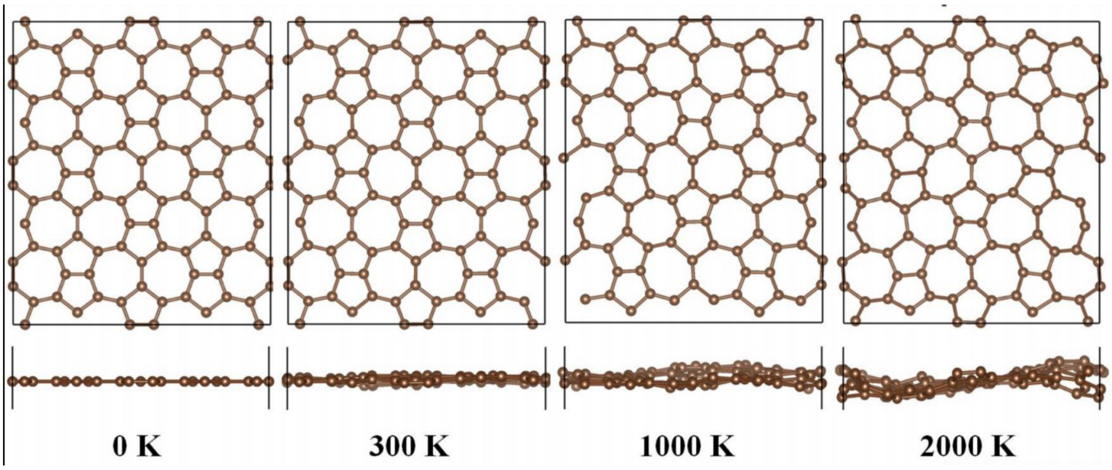

Figure 4

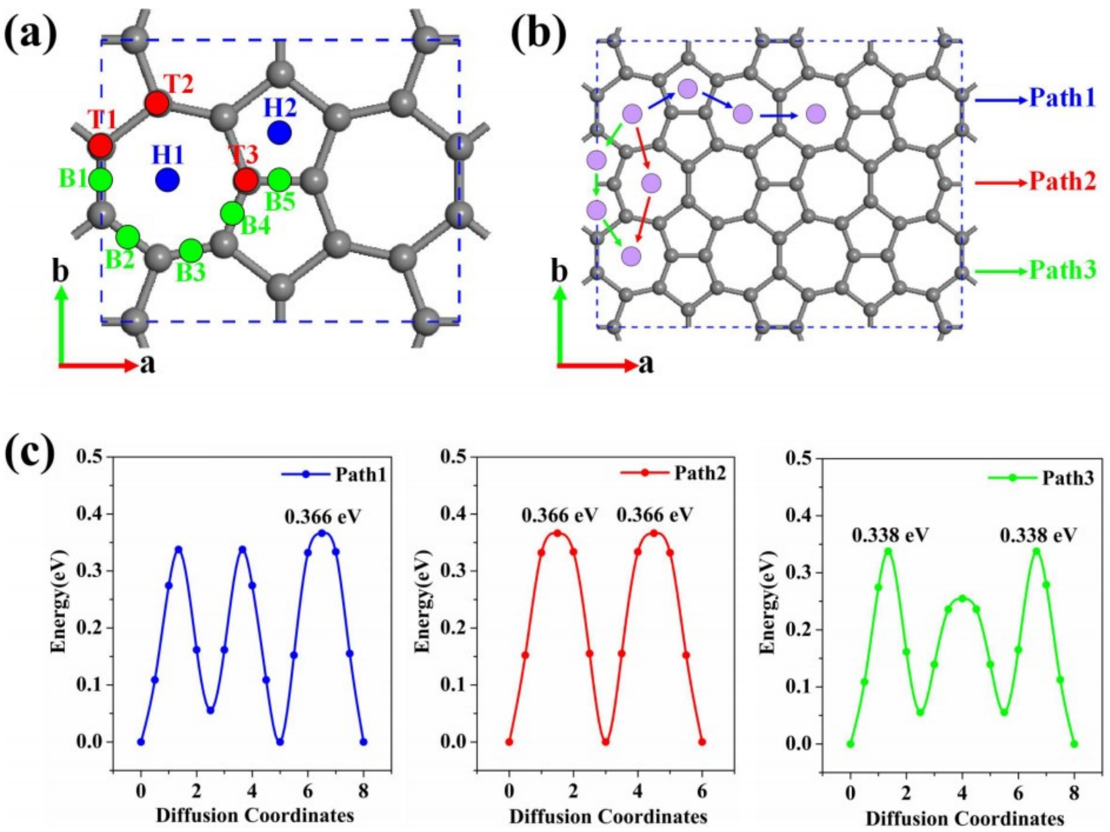
(a)
T1
T2
T3
H1
H2
B1
B2
B3
B4
B5
b
a
(b)
Path1
Path2
Path3
b
a
(c)
Path1
0.366 eV
Energy(eV)
Diffusion Coordinates
0.0
0.1
0.2
0.3
0.4
0.5
0
2
4
6
8
Path2
0.366 eV
0.366 eV
Energy(eV)
Diffusion Coordinates
0
2
4
6
Path3
0.338 eV
0.338 eV
Energy(eV)
Diffusion Coordinates
0
2
4
6
8

Figure 5